8

Autonomous Anthropomorphic Robotic System with Low-Cost Colour Sensors to Monitor Plant Growth in a Laboratory

Gourab Sen Gupta[1], Mark Seelye[1], John Seelye[2] and Donald Bailey[1]
[1]*School of Engineering and Advanced Technology (SEAT), Massey University, Palmerston North,*
[2]*The New Zealand Institute for Plant & Food Research Limited, Palmerston North New Zealand*

1. Introduction

An autonomous anthropomorphic robotic arm has been designed and fabricated to automatically monitor plant tissue growth in a modified clonal micro-propagation system which is being developed for the New Zealand Institute for Plant & Food Research Limited. The custom-fabricated robotic arm uses a vertical linear ball shaft and high speed stepper motors to provide the movements of the various joints, with the arm able to swivel 180 degrees horizontally. Sensors located at the end of the arm monitor plant growth and the ambient growing environment. These include a compact colour zoom camera mounted on a pan and tilt mechanism to capture high resolution images, RGB (red, green and blue) colour sensors to monitor leaf colour as well as sensors to measure ambient atmospheric temperature, relative humidity and carbon dioxide. The robotic arm can reach anywhere over multiple trays (600mm x 600mm) of plantlets. Captured plant tissue images are processed using innovative algorithms to determine tissue, or whole plant, growth rates over specified time periods. Leaf colour sensors provide information on the health status of tissue by comparing the output with predetermined optimum values. Custom software has been developed to fully automate the operation of the robotic arm and capture data, allowing the arm to return to specified sites (i.e. individual plantlets) at set time intervals to identify subtle changes in growth rates and leaf colour. This will allow plant nutrient levels and the immediate environment to be routinely adjusted in response to this continuous sensing, resulting in optimised rapid growth of the plant with minimal human input.
These low cost colour sensors can be incorporated into a continuous automated system for monitoring leaf colour of growing plants. Subtle colour changes can be an early indication of stress from less than optimum nutrient concentrations. In this chapter we also detail the calibration technique for a RGB sensor and compare it with a high end spectrophotometer.

2. Robotic systems in agriculture

Robotic and automated systems are becoming increasingly common in all economic sectors. In the past decade there has been a push towards more automation in the horticulture

industry, and it is only now, as robots become more sophisticated and reliable, that we are beginning to see them used to undertake routine, often repetitive tasks, which are expensive to do using a highly paid labour force. With rapid strides in technological advancement, more and more applications have become possible. These include the development of a robotic system for weed control (Slaughter, et al., 2008), a system for automatic harvesting of numerous agri-science products such as cutting flowers grown in greenhouses (Kawollek & Rath, 2008) and automating cucumber harvesting in greenhouses (van Henten, et al., 2002). Advances in electronics have empowered engineers to build robots that are capable of operating in unstructured environments (Garcia, et al., 2009). Camera-in-hand robotic systems are becoming increasingly popular, wherein a camera is mounted on the robot, usually at the hand, to provide an image of the objects located in the robot's workspace (Kelly, et al., 2000). Increasingly, robots are being used to sort, grade, pack and even pick fruits. Fruits can be identified and classified on a continuously moving conveyer belt (Reyes & Chiang, 2009). An autonomous wheeled robot has been developed to pick kiwifruit from orchard vines (Scarfe, et al., 2009). Robotic techniques for production of seedlings have been developed, identifying a need to add a machine vision system to detect irregularities in seed trays and to provide supplementary sowing using a 5-arm robot (HonYong, et al., 1999).

Automation of micro propagation for the rapid multiplication of plants has been described for the micro propagation of a grass species that replaces the costly and tedious manual process (Otte, et al., 1996). A system has also been developed that combines plant recognition and chemical micro-dosing using autonomous robotics (Sogaard & Lund, 2007).

Colour as a means of assessing quality is also gaining popularity amongst researchers. These include evaluating bakery products using colour-based machine vision (Abdullah, et al., 2000), monitoring tea during fermentation (Borah & Bhuyan, 2005), grading specific fruits and vegetables (Kang & Sabarez, 2009; Miranda, et al., 2007; Omar & MatJafri, 2009) and in the health sector to determine blood glucose concentrations (Raja & Sankaranarayanan, 2006). Near infrared (NIR) sensors are also gaining popularity as non-destructive means of assessing fruit and plant material, including the measurements of plant nutrient status (Menesatti, et al., 2010) as well as testing of fruit quality (Hu, et al., 2005; Nicola¨ı, et al., 2007; Paz, et al., 2009).

Investigation into non-destructive methods to measure the health status of plants is a relatively new area of research. Subtle leaf colour changes can be used as a measure of plant health. Although limited work has been carried out in real time, a recent micro-propagation based system used potato tissue images captured via a digital camera, to identify the colour of selected pixels (Yadav, et al., 2010). Spectral reflectance, using a range of spectral bands, has been used as a non-destructive measure of leaf chlorophyll content in a range of species (Gitelson, et al., 2003). Alternative methods make use of spectroscopic systems using a fixed light source to record colour reflectance of multiple samples (Yam & Papadakis, 2004).

The introduction of machine vision as a means of investigating the environment allows for very complex systems to be developed. Over the years the conventional "robotic design types" have remained more or less the same; however modified designs are increasingly being employed for specific tasks. Designs of robotic arms have made huge progress in recent years, as motor controllers, sensors and computers have become more sophisticated. It is envisaged that as more sensors, such as NIR (near infra-red) and colour sensors, become readily available, these will be integrated in the robotic arm. One such integrated system, which is unique and different from off-the-shelf robots, is detailed in this chapter.

3. Overview of the robotic system

The reported robotic system has been developed to work in a specific environment using specific sensors – it is meant to monitor growth of plant tissues in a laboratory. The plantlets are growing in multiple trays (600mm x 600mm) which are arranged contiguously on a shelf and there are multiple shelves one above the other. The robot should thus be able to extend its reach vertically and monitor plants in each shelf and be capable of reaching each tray. The robotic system designed is based on a SCARA (Selective Compliant Assembly/Articulated Robot Arm) robot. However, SCARA robots are rigid in the Z-axis and pliable in the XY-axes only. This rigidity in the Z-axis is a serious limitation of a SCARA robot for the given scenario. In the proposed system the entire arm is able to move in the Z-axis, as opposed to just the end-effector.

Another point of difference between the proposed system and conventional off-the-shelf industrial robot is the mechanism to house the sensors. To monitor the growth of plants, colour camera and RGB sensors are used. To enable the robot to position itself at a desired distance from the plant surface, proximity sensors are also required. The sensors need to be housed in an enclosure at the end of the robotic arm. In order to capture images and take RGB sensor readings from any angle it should be possible to pan and tilt the sensor housing structure. Such a mechanism is not a standard part of a conventional off-the-shelf industrial robot. In general, the costs of industrial robotic systems are far greater than the proposed system, often a lot more bulky and it is hard to integrate additional components (i.e. Sensors).

Two prototypes of the camera-in-hand robotic system were designed and built. The initial prototype made use of servo motors, designed as a simple experiment to test the viability of the system and its control mechanism. The colour camera was incorporated in this prototype and its control was implemented. The captured images were stored in a database for subsequent retrieval and processing. The prototype also helped to experiment with the wireless remote control of the robotic arm and the remote setting of camera features such as zoom, gain and exposure. Having established the 'proof-of-concept', the second prototype was designed and built to industrial specifications. This version of the prototype made use of high-torque stepper motors and greatly improved the performance of the robotic arm. Additionally, this prototype incorporated low-cost RGB colour sensors for monitoring plant health together with a proximity sensor. Sensors to monitor the ambient atmosphere were also incorporated to measure temperature, humidity and CO_2 levels. Section 3.1 gives a concise overview of the first prototype and section 3.2 details the second prototype in greater depth.

3.1 Robotic arm using servo motors

The basic concept of this robotic system, from human input to the control of the arm and camera, is outlined in the functional block diagram shown in figure 1. A system engineering approach was employed to take the robotic arm from concept to reality, making use of standard components and integrating them together to make the final product. The robotic arm was designed using 5 servo motors and implemented a pan and tilt mechanism for the camera.

The operator uses a joystick to control the movement of the robotic arm. This joystick connects to the PC via a USB interface. Movements of the joystick, made by the operator, vary the slide bars on the Graphical User Interface (GUI) running on the PC and at the same time control the movement of the joints of the arm. Serial data is then sent via the USB to the wireless transmitter (Zigbee Pro) module which transmits the data to the wireless receiver

module. The received data is then sent to the camera and the servo controller board. The user interface is shown in figure 2 and the completed robotic system, with plant trays, is shown in figure 3.

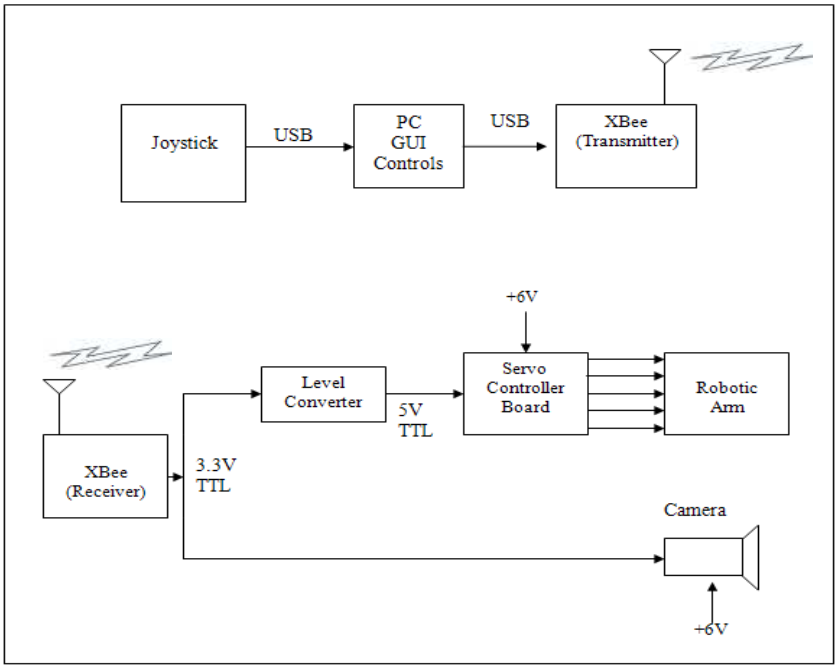

Fig. 1. Functional block diagram of the camera-in-hand robotic system

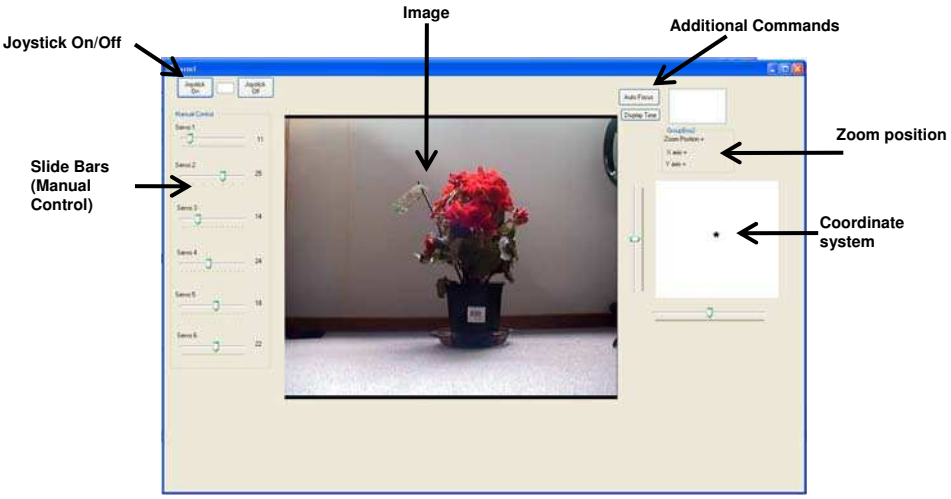

Fig. 2. The Graphical User Interface (GUI) of the robot control system

Fig. 3. The completed robotic arm with camera, joystick and plant trays

3.1.1 Control of servo motor based robotic arm

Using a modular approach the system was built and tested in parts. The sub-systems that had to be programmed, such as the servo-controller, joystick and camera, were tested separately. The testing setup and procedures are explained in this section. The servo controller board can take two types of serial mode signals – USB and 5V TTL UART. The controller board, together with the joystick, was tested using the connection diagram shown in figure 4.

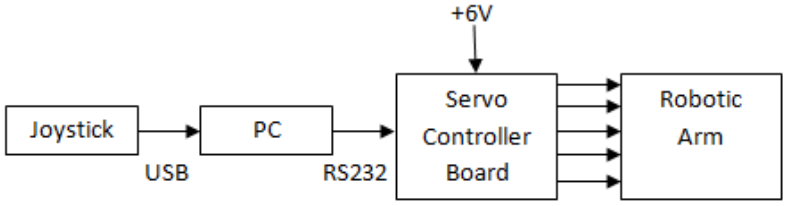

Fig. 4. Block diagram showing connection between PC, servo controller board and joystick

In the first instance a simple program was written in Visual Basic, allowing each servo motor to be controlled separately by clicking buttons. The motor parameters such as stepping rate and acceleration interval could be entered through the program's user interface. The user interface of the test program is shown in figure 5. This program sent the corresponding commands to the servo motor controller board. The next step was to control the servo motor by implementing a slide bar (figure 2). This allowed the operator to slide the bar, which incremented or decremented the position value, allowing simple movements based on the position byte. On successfully implementing controls for one servo motor, multiple servo motors could then be controlled in the same manner.

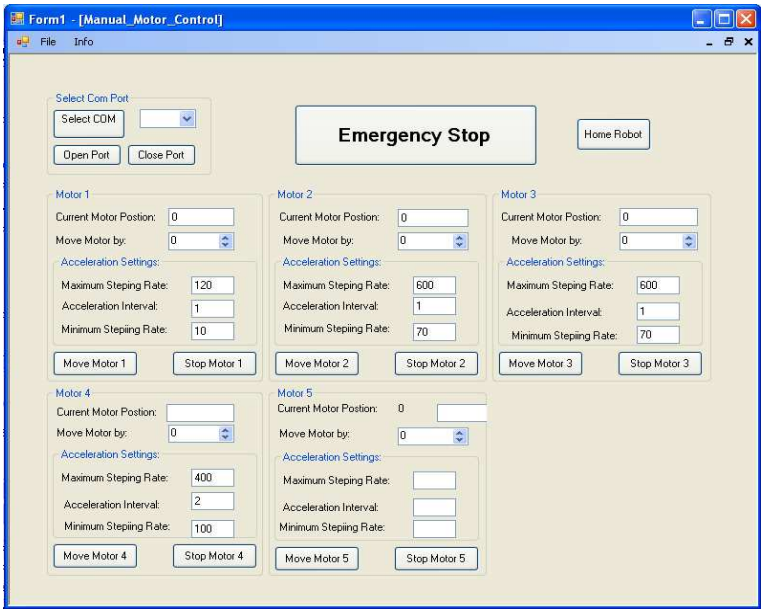

Fig. 5. User interface of the test program to control individual motors

3.2 Robotic arm using stepper motors

The second design of the robot was extensively influenced by the knowledge and insight gained from the servo motor based design of the robotic arm. The robotic arm was designed to move the end-effector over trays of plant material located on different levels of shelving units to capture images and the colour of the plant material and to use this information as a non-destructive measurement of plant health. To achieve this, a compact colour camera ("Sony Professional," 2010), proximity and colour sensor ("Parallax Home," 2010) are housed in the end-effector. Each tray measures approximately 600mm x 600mm, with each shelf located approximately 300mm above the previous shelf, with the top shelf approximately 1000mm high. The system is designed to move the arm into the trays, capture the required information and then move up to the next shelf and repeat the process on the next tray.

3.2.1 Mechanical design of the robotic arm

To allow the robotic arm to move vertically, a ball screw and shaft assembly is incorporated, converting rotational motion into vertical movement. The conceptual design is shown in figure 6. The arm contains a pan and tilt system at its distal end, which houses the camera, colour and proximity sensors. The operation of the arm is completely automated, continually gathering information from the sensors and capturing images for assessment and analysis.

The design is based on a modified SCARA robotic arm. Designed in the 3D CAD package, Solidworks, all components where machined in-house using a CNC machine. The arm itself has been through a number of design iterations to overcome unforeseen problems and to improve the efficiency of operation.

The robotic arm went through a number of design phases, with each design an improvement over the previous design iteration. In the initial concept it was intended to

Fig. 6. SolidWorks rendered design of the robotic arm

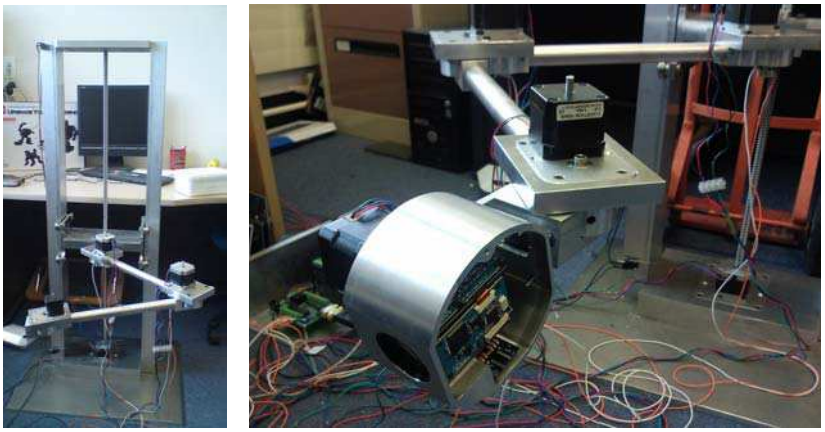

Fig. 7. The system in various stages of development and integration

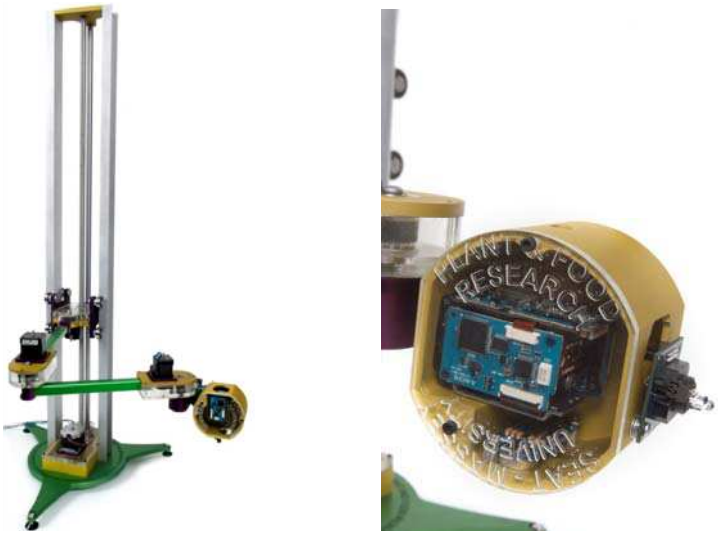

Fig. 8. (a) Completed robotic arm using stepper motors (b) Camera housing and RGB colour Sensors

make the links of the robotic arm extendable so that the robot can be flexible and adapted to operate in various workspaces. To ensure the motor torque ratings were not exceeded, a gearing system was investigated, which made use of spur gears to increase torque ratios. However, once constructed, a number of issues arose, including excessive weight (with the links extended) and slippage between gears. To overcome these issues a rethink of the arm design removed the ability to extend the link lengths, and a belt and pulley system was integrated to alleviate slippage within the gears. However, each design iteration maintained the overall original design concept. Figure 7 shows an initial version of the robotic arm in various stages of assembly and figure 8 shows the final design, with the various aluminium parts anodized. The completed robotic arm is shown in figure 8 (a). The close up view of the camera housing mechanism and the RGB colour sensors is shown in figure 8(b).

3.2.2 Actuation and control of the robotic arm joints using stepper motors

To allow the various joints to move, the arm uses bipolar, high torque stepper motors, which have varying amounts of torque, depending on the joint. The robotic arm uses five stepper motors that are controlled through a motor controller (KTA-190) and micro-step driver (M542) ("OceanControls," 2010). All the five motors have a step angle of 1.8 degrees and make use of a micro step driver that allows the user to select an even finer resolution (i.e. increasing the number of steps per revolution). Both a pulse signal and a direction signal are required for connecting a 4-wire stepper motor to the driver, with speed and torque depending on the winding inductance.

The KTA-190 motor controllers provide an interface between the computer and up to 4 stepper motors as well as the ability to control each motor independently or collectively. Utilizing a RS-232 9600, 8N1 ASCII serial communication protocol, up to 4 controller boards can be linked, giving control of up to 16 stepper motors (figure 9). A motor is controlled by a simple address, followed by the appropriate ASCII commands. The controller has as interface to allow limit switches to be used to prevent the motors from travelling out of range. With a total of 17 commands it is possible to tailor the operation and move the motors. Commands include: setting the position of the motors, returning the current positions of the motors, moving the motors by a relative or absolute amount and acceleration settings. A status command returns a 12-bit binary representation on the status of the controller board at any given time, providing information on the movement, direction and status of the limit switch respectively.

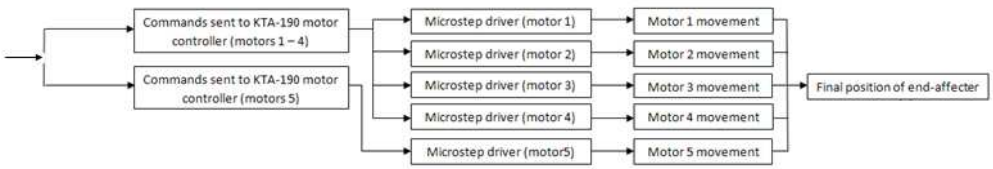

Fig. 9. Block diagram showing control of the 5 stepper motors

The angle each motor is required to move is calculated via an inverse kinematic algorithm. The user simply enters the desired tray that is required to be monitored, along with the number (and frequency) of readings within the tray. The software then calculates the required motor positions to enable the camera and sensors to capture the required

information. A proximity sensor has been integrated into the system to ensure that the colour readings are taken at a fixed height of 20mm above the plant material.

4. Sensors

Sensors provide information on the surroundings, which vary depending on their intended applications. A number of sensors have been integrated into the system to provide information in a non-destructive method on plant growth, with the intention of using low cost sensors which are easily amendable into the system. The use of a camera provides information on how fast the plant is growing, by identifying the quantity of plant material from a 2D view. Colour sensors provide information on the colour of an object. When colour sensors are used to monitor plant leaves, subtle changes can be detected before the human eye can identify them. This allows for media and nutrient levels to be adjusted accordingly. A proximity sensor ensures colour readings are taken at a fixed height, while temperature, humidity and CO_2 sensors provide information on the ambient environment.
We detail the camera control and testing in section 4.1. Colour sensor selection, along with calibration techniques and results, are presented in detail in section 4.2.

4.1 Camera

A Sony colour camera (model: FCB-IX11AP) was used. It features a ¼″ CCD (charge coupled device) image sensor using PAL (Phase Alternating Line) encoding system. The camera has a 40x zoom ratio (10x optical, 4x digital) that is controllable from a PC via Sony's VISCA (Video System Control Architecture) command protocol. Over 38,000 different command combinations are possible for controlling the cameras features. The camera's macro capability allows it to capture images as close as 10mm from the subject and it can operate in light conditions as low as 1.5 Lux. The electronic shutter speed is controllable from 1/10 to 1/10000 of a second allowing for clarity in photographs. In order for the camera's functions to be controlled, hexadecimal commands (as serial data) are sent to the camera. These serial commands require 8 data bits, 1 start bit, 1 (or 2) stop bit and no parity. They have a communication speed of 9.6, 19.2 or 38.4 kbps. The camera can be programmed and controlled using a TTL or RS232C signal level serial interface. To test the camera features, it was directly wired to the PC using the RS232C interface via a USB-to-RS232 converter as shown in figure 10. The video output signal from the camera was fed to a frame grabber/digitizer which is interfaced to the PC using USB. The image captured is displayed on the application's GUI (figure 12).

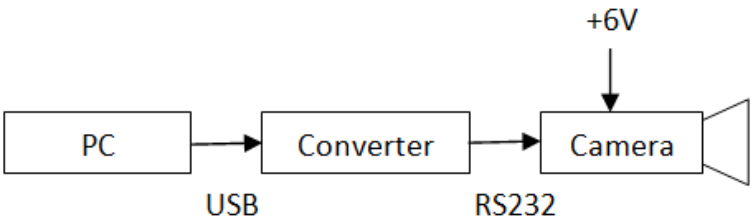

Fig. 10. Block diagram showing wired connection of PC to camera's RS232 inputs

To familiarize with the VISCA command structure and to test the various camera functions, especially the programming commands for controlling the zoom, a standard communication program (Terminal v1.9b) was used to send commands to the camera. To test the TTL interface, the system shown in figure 11 was employed. IC ST232 was used to convert the RS232 level signals to 5V TTL.

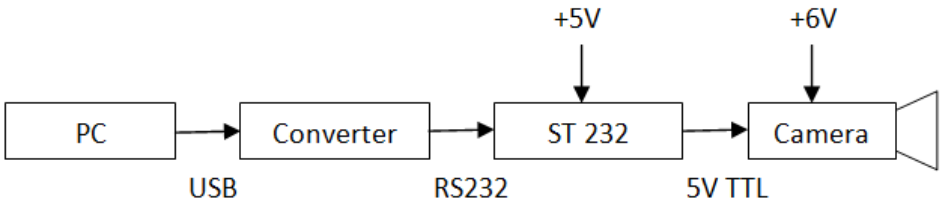

Fig. 11. Block diagram showing wired connection of PC to camera's TTL inputs

In the final design of the robotic system the camera was connected using the original RS-232 interface, with custom software created to control the features of the camera. Figure 12 shows the user interface which allows camera zoom, iris, gain, exposure settings and shutter features to be manually controlled. It also displays the image captured by the camera. Figure 13 shows the test program depicting the magnified image of the object under observation, with the camera set to 8x zoom.

Each of the controllable settings for the camera is controlled by sending arrays of hexadecimal commands to the camera, making use of Sony's VISCA protocol. Custom created software allows the user to control a number of settings to customize the camera to the user's desire.

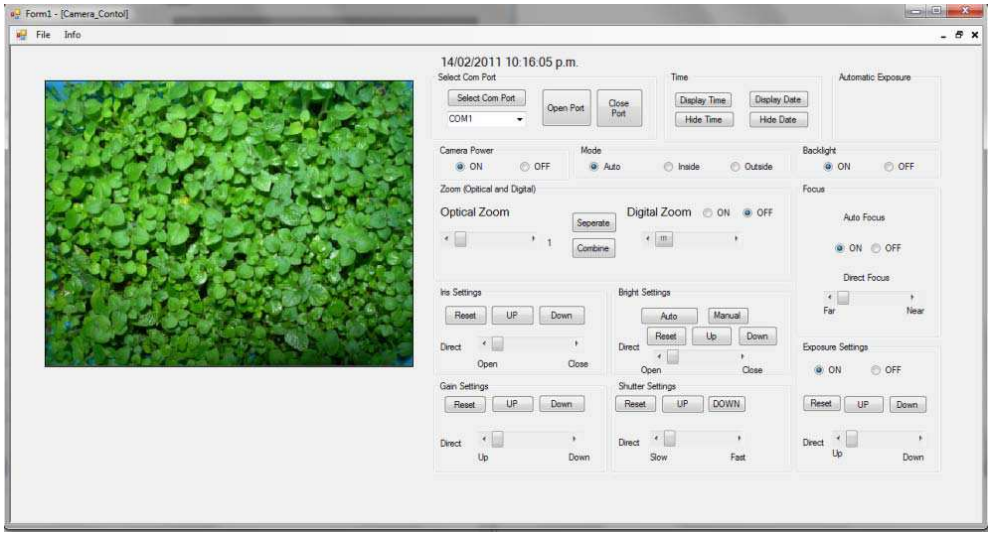

Fig. 12. User interface of the camera control program

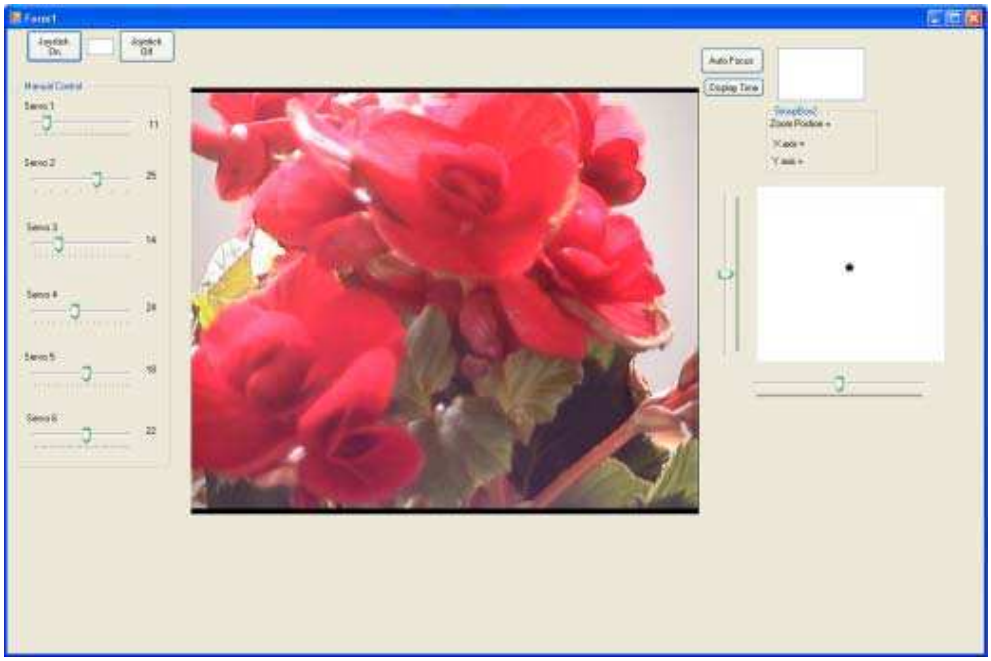

Fig. 13. Graphical User Interface (GUI) of the remote control application (camera zoom 8x)

4.2 RGB colour sensors

Currently there are a number of colour sensors on the market, with prices ranging from low cost light-to-frequency chips to sophisticated and very expensive spectrophotometers. Parallax (Parallax Inc, CA, USA) has two colour sensors that integrate seamlessly with their Basic Stamp microcontroller. Both the ColorPAL and TCS 3200 colour sensors are provided with some source code, making them amenable to integrating with our customised system.

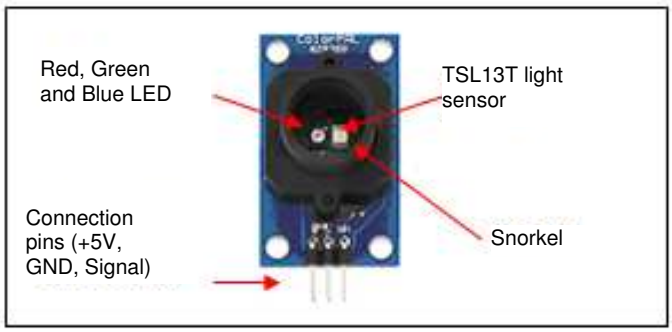

Fig. 14. Parallax ColorPAL colour sensor

The ColorPAL sensor (figure 14) illuminates a sample using in-built red, green and blue LED light sources (one colour at a time) and records the quantity of light reflected back from

the object. The ColorPAL makes use of a TAOS (Texas Advanced Optoelectronic Solutions) light-to-voltage chip. When light is reflected, the voltage, which is proportional to the light reflected, is used to determine the sample's R, G and B colour contents. The ColorPAL requires the sample to be illuminated using each of the red, green and blue LEDs, with a 'snorkel' to shield possible interference from external light sources. This requires the ColorPAL to be in direct contact with the object for an optimum reading without interference.

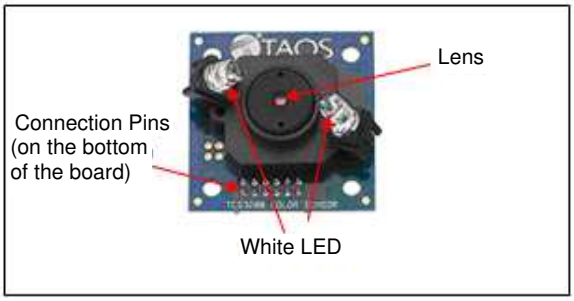

Fig. 15. Parallax TCS3200 colour sensor

The TCS3200 Colour sensor (figure 15) makes use of a TAOS TCS3200 RGB light-to-frequency chip. The TCS3200 colour sensor operates by illuminating the object with two white LEDs, while an array of photo detectors (each with a red, green, blue and clear filter) interpret the colour being reflected by means of a square wave output whose frequency is proportional to the light reflected. The TSC3200 Colour sensor has a 5.6-mm lens, which is positioned to allow an area of 3.5 mm^2 to be viewed.
A USB4000 spectrometer (Ocean Optics Inc., FL, USA) was used to find the height at which the greatest intensity of light occurred when the RGB sensor was placed above a sample. As the two white LEDs are directed down at an angle, there is a point where the light intensity is the greatest. This position was 20 mm above the surface of the sample, as shown in figure 16.

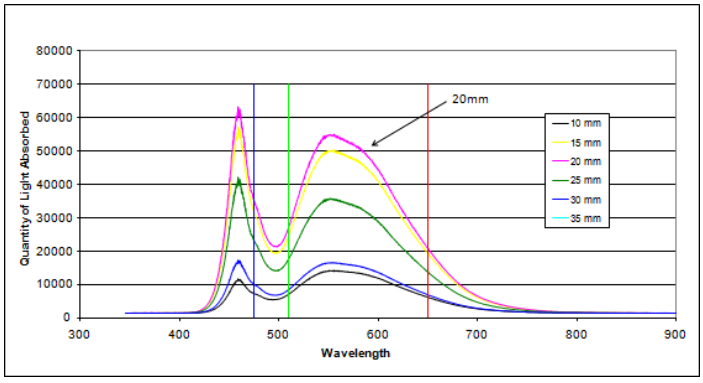

Fig. 16. Light absorbed from TCS3200 across the white LED light spectrum when the sensor is positioned at 6 different heights

Since the TCS3200 is mounted 20 mm above the sample, and therefore not in direct contact with the sample, it was more suited for our application than the full contact required by the ColorPAL sensor. A Konica Minolta CM-700D Spectrophotometer (Konica Minolta Sensing Americas, Inc., NJ, USA) was used to validate and calibrate the RGB sensors. For accurate measurements, the CM-700D was calibrated by taking both white and black readings by sampling a supplied white and black object respectively.
The CM-700D gives colour in the XYZ colour space, as well as L*a*b*, L*C*h, Hunter Lab, Yxy and Munsell. A linear transformation matrix was required to transform data from the XYZ colour space to the RGB colour space to enable comparisons and calibrations to the Parallax sensor. The linear transformation equation to be solved (Juckett, 2010) is:

$$\begin{pmatrix} X \\ Y \\ Z \end{pmatrix} = M \times \begin{pmatrix} R \\ G \\ B \end{pmatrix} \tag{1}$$

$$x = \frac{X}{X+Y+Z} \tag{2}$$

$$y = \frac{Y}{X+Y+Z} \tag{3}$$

$$z = \frac{Z}{X+Y+Z} \tag{4}$$

Equations (2 – 4) combined with the standard 1931 xy chromaticity diagram provided the foundation for the linear transformation (Eq. 1). This transformation converted the XYZ data initially to sRGB colour. The chromaticity values of x, y and z are shown in Table 1 (Lindbloom, 2010).

Colour	*x*	*y*	*z*
Red	0.64	0.33	0.212656
Green	0.30	0.60	0.715158
Blue	0.15	0.06	0.072186

Table 1. x, y, and z chromaticity values of red, green and blue converting xyz to sRGB

From the x, y and z chromaticity values (Table 1), the transformation matrix, M, is calculated (Eq. 5)

$$M \approx \begin{pmatrix} 0.721144 & 0.063298 & 0.166008 \\ 0.303556 & 0.643443 & 0.052999 \\ 0.000076 & 0.064689 & 1.024294 \end{pmatrix} \tag{5}$$

To calculate the R, G and B values the inverse is taken (Eq. 6 - 7).

$$\begin{pmatrix} R \\ G \\ B \end{pmatrix} = M^{-1} \times \begin{pmatrix} X \\ Y \\ Z \end{pmatrix} \tag{6}$$

$$M^{-1} \approx \begin{pmatrix} 1.436603 & -0.118534 & -0.226698 \\ -0.681279 & 1.618476 & 0.026671 \\ 0.042919 & -0.102206 & 0.974614 \end{pmatrix} \quad (7)$$

Colour	x	y	z
Red	0.7350	0.2650	0.176204
Green	0.2740	0.7170	0.812985
Blue	0.1670	0.0090	0.010811

Table 2. x, y, and z chromaticity values of red, green and blue converting xyz to CIE RGB

The x, y and z chromaticity values shown in Table 2, are again used to solve the transformation matrix, M (Eq. 8)
Testing showed that the TCS3200 produced light in the CIE RGB colour space, and although results would later show the colour sensor could be calibrated to the sRGB colour space, results from the calibration would be incorrect. Therefore a colour transformation to a CIE RGB colour space was more appropriate than the sRGB colour space; consequently a new linear transformation was required.

$$M \approx \begin{pmatrix} 0.4887180 & 0.3106803 & 0.2006017 \\ 0.1762044 & 0.8129847 & 0.0108109 \\ 0.0000000 & 0.0102048 & 0.9897952 \end{pmatrix} \quad (8)$$

Again calculating the R, G and B values the inverse is taken (Eq. 6).

$$M^{-1} \approx \begin{pmatrix} 2.3706743 & -0.9000405 & -0.4706338 \\ -0.5138850 & 1.4253036 & 0.0885814 \\ 0.0052982 & 0.0052982 & 1.0093968 \end{pmatrix} \quad (9)$$

4.2.1 Colour sensor calibration and results

In order to validate the TCS3200 colour sensor, it was necessary to calibrate and test it using the CM-700D Spectrophotometer. This involved taking 200 RGB readings with the TCS3200 using fifteen different coloured samples from the Royal Horticulture Society (RHS) colour charts and averaging them. The same samples were measured, each 20 times, with the CM-700D and again averaged. These tests were all completed in a constant temperature dark room. As the CM-700D uses the XYZ colour space, the linear transformation matrix was used to convert the XYZ values to a CIE RGB colour space (Eq. 9).
The TCS3200 was firstly calibrated through software by modifying the integration time, to allow the white object (used to calibrate the CMD-700) to have a RGB value as close as possible to 255,255,255 followed by scaling each of the RGB values, to ensure the white reading was that of the CMD-700.
In order to calculate a calibration factor the following equation was used:

$$R_N^{'} = R_N^{\gamma} \quad (10)$$

where: $R_N^{'}$ = CM-700D (desired RGB value)

R_N = TCS3200 RGB (Un-calibrated sensor data)

γ = Gamma (required calibration factor)

First the TCS3200 sensor data were scaled to ensure all values are offset, thus ensuring that the white reading is that of the CMD-700 for each of R, G and B reading (Eq. 11)

$$R_N = R \times \frac{R_N^{'}}{R_{\max}}, G_N = G \times \frac{G_N^{'}}{G_{\max}}, B_N = B \times \frac{B_N^{'}}{B_{\max}} \tag{11}$$

where $R_{\max}, G_{\max}, B_{\max}$ represent the maximum R, G and B value of a white object from the TCS3200.

ID	TCS-3200						CMD-700			Output Calibrated		
	Gain Adjusted			White Adjusted			RGB Equivalent (CIE)					
	R	G	B	R	G	B	R	G	B	R	G	B
123A	99	148	167	88	152	144	62	155	152	85	158	143
127C	38	79	75	34	81	65	17	89	69	31	89	64
129C	99	152	137	88	156	118	71	166	123	85	162	117
131C	25	41	35	22	42	30	10	43	27	20	49	29
133C	62	88	85	55	90	73	47	93	80	52	98	72
135C	42	51	35	37	52	30	36	78	39	35	60	29
137C	42	51	35	37	52	30	40	54	30	35	60	29
139C	68	82	58	61	84	50	63	88	48	57	92	49
141C	57	80	45	51	82	39	55	87	35	48	90	38
143C	71	88	48	63	90	41	72	91	32	60	98	41
145C	171	168	122	152	172	105	169	185	101	149	178	104
147C	84	86	62	75	88	53	84	91	51	71	96	53
149C	174	183	114	155	187	98	170	206	86	152	192	97
155D	255	249	258	227	255	222	227	255	222	226	255	222
202A	17	17	20	15	17	17	10	13	13	14	22	17

Table 3. Results obtained comparing the TCS3200 colour sensor (calibrated and un-calibrated) with the CM-700D spectrophotometer over a range of 15 RHS colours

Table 3 shows the data recorded from the colour sensors along with the equivalent results from the CMD-700 (using the CIE RGB transformation matrix) and the calibrated TCS3200 results. Table 4, shows the errors associated with the Table 3.

The calibration factors (γ) for each colour were calculated using normalized data. (Eq. 12)

$$\gamma_R = \frac{\log(R_N^{'} / 255)}{\log(R_N / 255)}, \gamma_G = \frac{\log(G_N^{'} / 255)}{\log(G_N / 255)}, \gamma_B = \frac{\log(B_N^{'} / 255)}{\log(B_N / 255)} \tag{12}$$

For each colour sample measured, the calibration factor was calculated and averaged using a geometric mean (as opposed to the more general arithmetic mean function (Fleming &

Wallace, 1986), thus providing the γ factor for R, G and B individually. The (desired) calibrated values were then obtained using equation 13.

$$R'_{N(calibrated)} = (R_N / 255)^{\gamma} \times 255 \tag{13}$$

For a range of fifteen colours, measurements were taken using the TCS3200 RGB sensor and the CM-700D Spectrophotometer (Table 3). The gamma calibration factors calculated were:

$$(\text{Red})\lambda_R = 1.05,\ (\text{Green})\lambda_G = 0.92,\ (\text{Blue})\lambda_B = 1.00 \tag{14}$$

	TCS3200 (un-calibrated)			TCS3200 (calibrated)		
Colour	R	G	B	R	G	B
Error	9.691	6.806	5.107	10.161	6.162	4.966
Error %	3.8	2.669	2.003	3.985	2.416	1.947
S.D	7.423	7.298	3.485	6.631	4.757	3.699

Table 4. Average Error (0-255), percentage error and standard deviation for red, green and blue measurements of the TCS3200 colour sensor, calibrated and un-calibrated, compared with CM-700D spectrophotometer results across a range of colours

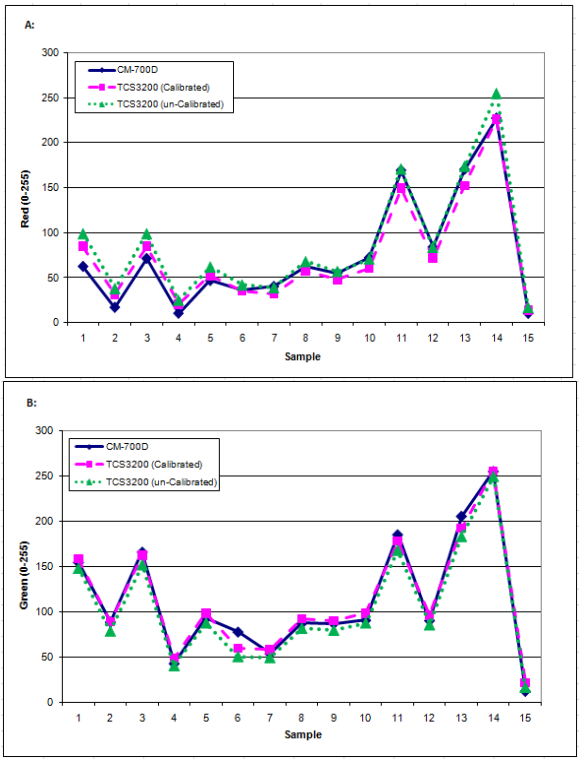

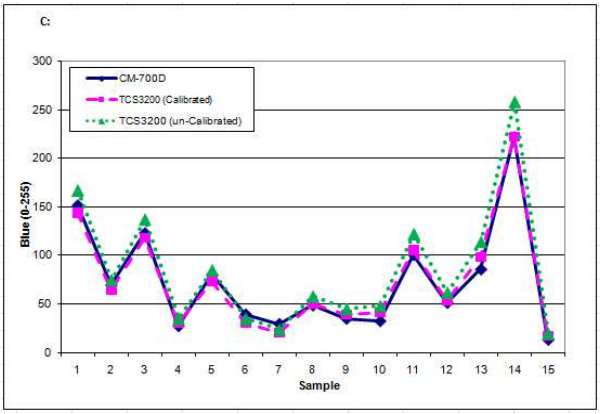

Fig. 17. TCS3200 sensor RGB readings, calibrated and un-calibrated, compared with the CM-700D readings of: Red (A); Green (B); Blue (C) using a CIE RGB colour transformation. (Colour samples are as given in Table 3)

An example of a green colour interpreted by the CM-700D and TCS3200 colour sensor before and after calibration is shown in figure 18.

TCS3200 (un-calibrated)	TCS3200 (calibrated)	CM-700D Spectrophotometer
RGB = 63,90,41	RGB = 60,98,41	RGB = 72,91,32

Fig. 18. Graphical representation of the colour differences between, calibrated and un-calibrated TCS3200 colour sensor

Results showed when calibrating the CM-700D XYZ values to CIE RGB instead of sRGB, the calibration results improved, as shown in Table 5, to have a much smaller error for R, G and B. A colour representation can be seen in Figure 19.

	CIE RGB			sRGB		
Colour	R	G	B	R	G	B
Error	10.289	6.117	5.683	14.777	7.055	9.564
Error %	4.035	2.399	2.229	5.795	2.767	3.751
S.D	6.562	4.739	3.357	12.314	7.54	5.772

Table 5. Comparisons between CIE RGB and sRGB transformation matrix, showing the CIE RGB results to be more accurate than the sRGB

TCS3200 (raw reading)	CM-700D Spectrophotometer (sRGB)	CM-700D Spectrophotometer (CIE RGB)
RGB 71,88,48	RGB = 149,166,81	RGB = 72,91,31
		

Fig. 19. An example of a green colour interpreted by the TCS3200 colour sensor with no calibration compared with the CM-700D with both a sRGB and CIE RGB

5. Conclusion

An anthropomorphic robotic arm has been designed, fabricated and fully tested to meet the requirements set out by The New Zealand Institute for Plant & Food Research Limited. The robotic system is able to reach and monitor plantlets growing in trays on a multi-level shelving unit. Custom software has been developed to fully automate the control of the robotic arm. The position of the robotic arm can be controlled with great precision using the microstepper controller to allow micro-motion of the stepper motors. The robot can be programmed to autonomously position itself and take readings at regular intervals.

Several sensors have been integrated in the robotic system, namely a high-end colour camera for capturing high resolution images of plantlets; proximity sensor to position the arm at a predetermined distance from the plant surface for taking measurements; temperature, humidity and CO_2 sensors to monitor the ambient atmospheric conditions and a low-cost RGB sensor to measure the colour of plant leaves.

Two different RGB sensors have been evaluated. Experimental results show that the Parallax TCS3200 RGB sensor is a useful low cost colour sensor, which when calibrated to an industry standard spectrophotometer, can provide accurate RGB readings. It is therefore a useful component for integrating into an automated system such as a robotic arm, with various other sensors, for monitoring plants growing in a modified plant micro-propagation system.

The system has the potential for not only monitoring plant material in a laboratory environment but other applications as well where non-destructive measurements of colour are required.

6. Acknowledgment

The hardware cost of this research has been funded by The New Zealand Institute for Plant & Food Research. The authors greatly appreciate the financial and technical workshop support given by the School of Engineering and Advanced Technology, Massey University and The New Zealand Institute for Plant & Food Research Limited.

7. References

Abdullah, M. Z., Aziz', S. A., & Mohamed, A. M. D. (2000). Quality Inspection Of Bakery Products Using A Color-Based Machine Vision System. Journal of Food Quality, 23 (1), 39-50.

Borah, S., & Bhuyan, M. (2005). A computer based system for matching colours during the monitoring of tea fermentation. International Journal of Food Science and Technology, 40(6), 675-682.

Lindbloom, B. (2010). Useful colour Equations. Retrieved 18/8/2010, from http://www.brucelindbloom.com/

Fleming, P. J., & Wallace, J. J. (1986). How not to lie with statistics: The correct way to summarize the benchmark results. Communications of the ACM, 29(3), 218-221

Garcia, G. J., Pomares, J., & Torres, F. (2009). Automatic robotic tasks in unstructured environments using an image path tracker. Control Engineering Practice, 17(5), 597-608.

Gitelson, A. A., Gritz, Y., & Merzlyak, M. N. (2003). Relationships between leaf chlorophyll content and spectral reflectance and algorithms for non-destructive chlorophyll assessment in higher plant leaves. Journal of Plant Physiology, 160(3), 271-282.

HonYong, W., QiXin, C., Masateru, N., & JianYue, B. (1999). Image processing and robotic techniques in plug seedling production. Transactions of the Chinese Society of Agricultural Machinery, 30, 57-62.

Hu, X., He, Y., Pereira, A. G., & Gómez, A. H. (2005). Nondestructive Determination Method of Fruit Quantity Detection Based on Vis/NIR Spectroscopy Technique. 27th Annual International Conference of the Engineering in Medicine and Biology Society (IEEE-EMBS 2005), 1956-1959

Juckett, R. (2010). RGB color space conversion - Linear transformation of color. Retrieved 14/8/2010, from http://www.ryanjuckett.com

Kang, S. P., & Sabarez, H. T. (2009). Simple colour image segmentation of bicolour food products for quality measurement. Journal of Food Engineering, 94, 21-25.

Kawollek, M., & Rath, T. (2007). Robotic Harvest of Cut Flowers Based on Image Processing by Using Gerbera jamesonii as Model Plant. In S. DePascale, G. S. Mugnozza, A. Maggio & E. Schettini (Eds.), Proceedings of the International Symposium on High Technology for Greenhouse System Management (Greensys 2007), 557-563

Kelly, R., Carelli, R., Nasisi, O., Kuchen, B., & Reyes, F. (2000). Stable Visual Servoing of Camera-in-Hand Robotic Systems. IEEE/ASME Transactions on Mechatronics, 5(1), 39 - 48.

Menesatti, P., Antonucci, F., Pallottino, F., Roccuzzo, G., Allegra, M., Stagno, F., et al. (2010). Estimation of plant nutritional status by Vis–NIR spectrophotometric analysis on orange leaves. Biosystems Engineering, 105(4), 448-454.

Miranda, C., Girard, T., & Lauri, P. E. (2007). Random sample estimates of tree mean for fruit size and colour in apple. Scientia Horticulturae, 112 (1), 33-41.

Nicola¨ı, B. M., Beullens, K., Bobelyn, E., Peirs, A., Saeys, W., Theron, K. I., et al. (2007). Nondestructive measurement of fruit and vegetable quality by means of NIR spectroscopy: A review. Postharvest Biology and Technology, 46(2), 99-118.

OceanControls. (2010). Retrieved 12/04/2010, from www.oceancontrols.com.au

Omar, A. F. B., & MatJafri, M. Z. B. (2009). Optical Sensor in the Measurement of Fruits Quality: A Review on an Innovative Approach. International Journal of Computer and Electrical Engineering, 1(5), 557-561.

Otte, C., Schwanke, J., & Jensch, P. (1996). Automatic micropropagation of plants. Optics in Agriculture, Forestry, and Biological Processing II, Proc. SPIE 2907, 80-87.

Parallax Home. (2010). Retrieved 05/07/2010, from www.Parallax.com

Paz, P., S´anchez, M. ı.-T., P´erez-Mar´ın, D., Guerrerob, J. e.-E., & Garrido-Varob, A. (2009). Evaluating NIR instruments for quantitative and qualitative assessment of intact apple quality. Journal of the Science of Food and Agriculture, 89(5), 781-790.

Raja, A. S., & Sankaranarayanan, K. (2006). Use of RGB Color Sensor in Colorimeter for better clinical measurements of blood Glucose. BIME Journal 6(1), 23 - 28.

Reyes, J., & Chiang, L. (2009). Location And Classification Of Moving Fruits In Real Time With A Single Colour Camera. Chilean Journal Of Agricultural Research, 69, 179-187.

Scarfe, A. J., Flemmer, R. C., Bakker, H. H., & Flemmer, C. L. (2009). Development of An Autonomous Kiwifruit Picking Robot. 4th International Conference on Autonomous Robots and Agents, 380-384.

Slaughter, D. C., Giles, D. K., & Downey, D. (2008). Autonomous robotic weed control systems: A review. Computers and Electronics in Agriculture, 61(1), 63-78.

Sogaard, H. T., & Lund, I. (2007). Application accuracy of a machine vision-controlled robotic micro-dosing system. biosystems engineering, 96(3), 315-322.

Sony Professional. (2010). Retrieved 05/06/2009, from www.pro.sony.eu

van Henten, E. J., Hemming, J., van Tuijl, B. A. J., Kornet, J. G., Meuleman, J., van Os, E. A., et al. (2002). An autonomous robot for harvesting cucumbers in greenhouses. [Article]. Autonomous Robots, 13(3), 241-258.

Yadav, S. P., Ibaraki, Y., & Gupta, S. D. (2010). Estimation of the chlorophyll content of micropropagated potato plants using RGB based image analysis. Plant Cell Tissue and Organ Culture, 100(2), 183-188.

Yam, K. L., & Papadakis, S. E. (2004). A simple digital imaging method for measuring and analyzing color of food surfaces. Journal of Food Engineering, 61, 137-142.

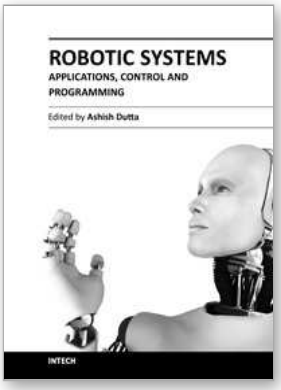

Robotic Systems - Applications, Control and Programming
Edited by Dr. Ashish Dutta

ISBN 978-953-307-941-7
Hard cover, 628 pages
Publisher InTech
Published online 03, February, 2012
Published in print edition February, 2012

This book brings together some of the latest research in robot applications, control, modeling, sensors and algorithms. Consisting of three main sections, the first section of the book has a focus on robotic surgery, rehabilitation, self-assembly, while the second section offers an insight into the area of control with discussions on exoskeleton control and robot learning among others. The third section is on vision and ultrasonic sensors which is followed by a series of chapters which include a focus on the programming of intelligent service robots and systems adaptations.

INTECH
open science | open minds

InTech Europe
University Campus STeP Ri
Slavka Krautzeka 83/A
51000 Rijeka, Croatia
Phone: +385 (51) 770 447
Fax: +385 (51) 686 166
www.intechopen.com

InTech China
Unit 405, Office Block, Hotel Equatorial Shanghai
No.65, Yan An Road (West), Shanghai, 200040, China
中国上海市延安西路65号上海国际贵都大饭店办公楼405单元
Phone: +86-21-62489820
Fax: +86-21-62489821